14

Vibration Analysis of an Oil Production Platform Submitted to Dynamic Actions Induced by Mechanical Equipment

José Guilherme Santos da Silva, Ana Cristina Castro Fontenla Sieira
Luciano Rodrigues Ornelas de Lima and Bruno Dias Rimola
State University of Rio de Janeiro (UERJ)
Brazil

1. Introduction

Structural engineers have long been trying to develop solutions using the full potential of its composite materials. At this point there is no doubt that the structural solution progress is directly related to an increase in materials science knowledge.

On the other hand, the competitive trends of the world market have long been forcing structural engineers to develop minimum weight and labour cost solutions. A direct consequence of this new trend design is a considerable increase in problems related to unwanted floor vibrations. For this reason, the structural floors systems can become vulnerable to excessive vibrations, for example, produced by impacts such as mechanical equipment (rotating machinery) (Rimola, 2010; Rimola, 2010a; Rimola, 2010b).

This way, the present paper investigated the dynamic behaviour of an oil production platform made of steel and located in Santos basin, São Paulo, Brazil. The structural model consists of two steel decks with a total area of 1915 m² (upper deck: 445 m² and lower deck: 1470 m²), supported by vertical sections made of tubular steel members (steel jacket), and piled into the seabed. A variety of mechanical equipment was located on the steel decks of the structural model, related to electrical generators and compressors (Rimola, 2010).

The soil representation was based on the Winkler's Theory (Winkler, 1867). This theory simulates the soil behaviour as a group of independent springs, governed by the linear-elastic model. In the Winkler's model, the soil stiffness was considered as the necessary pressure to produce a unitary displacement (Winkler, 1867).

The proposed computational model, developed for the oil production platform dynamic analysis, adopted the usual mesh refinement techniques present in finite element method simulations implemented in the GTSTRUDL program (GTSTRUDL, 2009). In this finite element model, floor steel girders and columns were represented by three-dimensional beam elements, where flexural and torsion effects were considered. The steel decks were represented by shell finite elements. In this investigation, it was considered that both structural elements (steel beams and steel deck plates) have total interaction with an elastic behaviour.

The structural model dynamic response was determined through an analysis of its natural frequencies and peak accelerations. The results of the dynamic analysis were obtained from

an extensive numerical study, based on the finite element method using the GTSTRUDL program (GTSTRUDL, 2009). In this investigation, dynamic loadings coming from the rotating machinery (electrical generators and compressors) were applied on the steel decks of the structural system (production platform).
A numerical analysis was performed, in order to obtain the dynamic impacts on the deck structure coming from the electrical generators and compressors. Based on the peak acceleration values, obtained on the structure steady-state response, it was possible to evaluate the structural model performance in terms of human comfort, maximum tolerances of the mechanical equipment and vibration serviceability limit states of the structural system, based on the design code recommendations (CEB 209/91, 1991; ISO 1940-1, 2003; ISO 2631-1, 1997; ISO 2631-2, 1989; Murray et al., 2003).

2. Vibration analysis of steel floors

Besides the evaluation of the structural systems behaviour when submitted to dynamic loads, the causes and effects of vibration on people have been subject of many studies and experiments, due to the fact that they affect people in different ways, causing discomfort, health problems, reduced ability concentration and efficiency at work or sickness, in the case of vibrations of very low frequencies.
(Reiher & Meister, 1946) developed a scale used to determine levels of acceptable vibration in floors. This scale was developed based on experiments in which a group of people was submitted to vibration, whose frequency varied from 1 Hz to 100 Hz. According to this scale, the vibration levels can be classified into several levels, depending on the amplitude and frequency.
(Srinivasulu & Vaidyanathan, 1976) presented the principles of analysis, design and construction of machines of different types. The authors investigated several factors to be considered during the design of machine foundations, in order to obtain the best solution, leading to better operation and reduce the undesirable effects of vibrations on the structure.
(Bachmann & Ammann, 1987) have studied the necessary procedures for the analysis of structures under dynamic loads coming from machines, including machines with rotating parts. The authors treat from the load formulation, also dealing with the effects of machinery induced vibrations in structures and measures to avoid such a problem. In their work are also included the acceptance criteria, both from the point of view of the structure and the point of view of human comfort.
(Griffin, 1996) indicates some reasons to measure human exposure to vibration, especially the following: development of standardized documentation on vibrations in the human body; determination of vibration levels and reduction in frequency range that can prejudice the human body and providing data that may be used for comparison between two or more occupational environments.
(Lenzen, 1996) observed during the development of his research, that the scale developed by (Reiher & Meister, 1946) did not take into account the influence of damping on the human perception of vibration. Through his studies in the laboratory, it was modified the scale of (Reiher & Meister, 1946). This modified scale showed satisfactory results in floors with damping ratios of up to 5%.
According to (Vasconcelos, 1998), establishing the concept of human vibration discomfort can be a difficult task. There are several factors that can influence the subjective feeling of discomfort, such as the socio-cultural people, the type of activity performed, the person's

psychological state at the time of the event, environmental factors, noise, etc. It is not easy to simulate these conditions in the laboratory to reduce the variability of individual responses. Thus, the limit of comfort of people subjected to vibration can be regarded as a rather subjective measure, generating some controversy as to the acceptable values of accelerations imposed.

(Zhou & Shi, 2001) considered that the elimination of vibration of rotating machinery is an important engineering problem. In their study, they presented a detailed review of the developed research that deals with the active balancing of rotors in real time and active control of vibration of rotating machinery, as well as dynamic modelling and analysis techniques for rotating systems. The authors report that the major problem found by the scheme of active control of vibration is the limited number of actuators to control an unlimited number of vibration modes.

(Pereira, 2005) presents a study on the vibration related to human comfort and perception, focusing on the suitability of buildings for vibration levels, aiming the generation of curves related to the perception and human comfort and vibration by means of laboratory experiments and comparing the results to the limits of vibration to other investigations and the design codes (ISO 2631-2, 1989).

The experimental tests developed by (Pereira, 2005) considered 30 volunteers, 15 men and 15 women exposed to vertical vibration at a frequency band ranging from 12 to 80 Hz in sitting and standing posture. The author also performed an analysis on the uncertainty of the outcome of the limit of perception, verifying the existence of a range of vibration in which individuals are not sure whether or not they are able to detect the vibration. It also aimed to know the vertical vibration levels that people find uncomfortable at their home environment, to determine the relationship between the perception threshold and comfort. According to these results, it was proved that the reduction in amplitude of the movement to higher frequency vibration becomes more difficult to be detected, reducing the sensitivity of people.

(Milet, 2006) discusses the basic concepts of dynamic analysis of machine foundations, investigating some analytical strategies and numerical methods available for designing. In this work, some design recommendations were presented and discussed.

(Souza et al., 2007) developed a prototype that allows, looking through a simple system, based on an unbalanced rotor, possible structural data caused by the resonance phenomenon, also allowing comparisons to be made with more complex structural systems. Furthermore, the experiment presented as being practical and simple, can serve as an analytical tool in the classroom, thus giving a better understanding of phenomena related to the vibration system.

(Assunção, 2009) addressed the issues and the most important conditions for a dynamic analysis of elevated frame structures, where equipment were allocated for industrial processes. The author developed a study related to the main causes of dynamic actions coming from industrial equipment and examined a framed structure supporting an unbalanced machine. Through this investigation, the author demonstrated that the developed computational model was appropriate to simulate the transmission of efforts and contribution of the vibrating mass on the responses of the framed structures.

3. Loads generated by mechanical equipment (rotating machinery)

Knowledge about the dynamic behaviour of rotors of rotating machinery, even in the design phase, has become an increasingly crucial factor, considering that it is not desirable to take

corrective actions after the beginning of activities. Material costs and delivery of services are relatively high when compared with the profits increasingly reduced according to the rules imposed by the market and the fact that such corrective actions still involve a period in which the equipment will need to become inoperative, which means losses, because it will not generate any profit for the period.

According to (Dias Junior, 2009), among several factors that contribute to the transmission of rotational energy to the vibratory movements of the machine, the well-known is undoubtedly the unbalance of the rotor. The rotor is the rotating part of a machine or engine which may be coupled elements as disks, generators, gears, etc. According to (Dias Junior, 2009), due to the unbalance, the force that acts at the rotor gravity centre, pull the shaft out of the line joining the two bearings, forcing the shaft to rotate stressed. This movement is called precession movement.

Rotors are supported on bearings, which are the elements responsible for connecting the movable and fixed structure of a rotating machine. In addition to this point, to absorbing energy, another function of the bearings is to guide or restrict movement during the rotation axis (Silva, 2004).

The process of balancing a rotor is a key factor to minimize the vibrations generated by electric motors. Depending on the vibration level of these engines, the structural system that supports the equipment can be compromised by fatigue or even premature failure. The balancing process is intended to improve the distribution of mass of a body, so that by turning around their bearings, produces no unbalance forces, keeping the vibrations and dynamic loads within suitable limits for the machine operation.

The balance can be achieved up to a certain limit, since after this process the rotor still presents imperfection in the mass distribution, called residual unbalance. It is worth mentioning that there is a direct relationship between the residual unbalance and vibration level of the machine, which depends on many factors (mass housing and the foundation, stiffness of the bearings and foundation, occurrence of resonances etc.). Anyway, there are allowable levels of residual unbalance, consistent with good practice of machine design.

3.1 Excitation forces: Unbalanced mass

Unbalanced mass is defined as a mass located at a distance d measured from the geometric centre of the shaft. The mass remains in a plane perpendicular to the axis y and it is a constant coordinate, as illustrated in Figure 1.

Based on Figure 1, it can be deduced that the force caused by unbalanced mass, acting on the axis, according to directions in the shown coordinate system, can be written as presented in Equations (1) and (2). In Equations (1) and (2), the dynamic forces generated by unbalanced mass have a frequency similar to the rotational frequency of the axis

$$F_u = m_u \Omega^2 d \cdot \sin(\Omega t) \tag{1}$$

$$F_w = m_u \Omega^2 d \cdot \cos(\Omega t) \tag{2}$$

3.2 Unbalance quantification

As previously mentioned, the unbalance is characterized by a mass located at a certain distance from the rotation axis, see Figure 1. Therefore, the unbalance is always measured by a product mass x distance, see Equation (3). The rotor must be subjected to a balancing

procedure, in order to achieve a tolerable minimum. This value is called the Permissible Residual Unbalance and designated by the symbol U.

$$U = \text{mass} \times \text{distance} \tag{3}$$

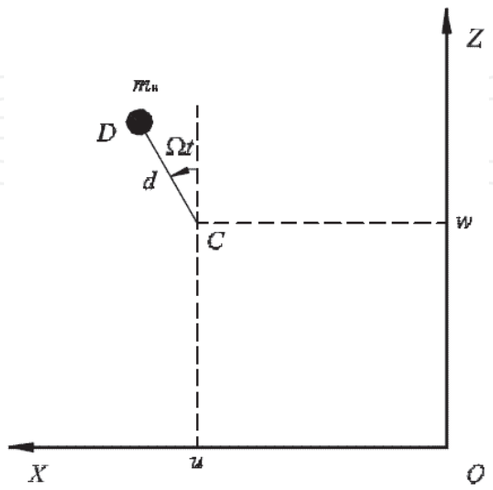

Fig. 1. Unbalanced mass (López, 2002)

It was observed in Equation (3), that the allowable residual unbalance is directly proportional to the mass of the rotor, i.e., as heavier was the rotor, greater it will be the permissible residual unbalance. It is appropriate to relate the allowable residual unbalance, U, and the rotor mass, m, in terms of the Specific Allowable Residual Unbalance, as shown in Equation (4).

$$e = \frac{U}{m} \tag{4}$$

As larger is the rotation speed, smaller should be the residual unbalance, since the centrifugal force, F_{cent}, increases with the square of the speed of it, as shown in Equation (5). In Equation (5) the centrifugal force, F_{cent} is expressed in N.

$$F_{cent} = m \cdot e \cdot \Omega^2 \tag{5}$$

Based on many years of experience, experts decided that the product of the angular velocity of rotor rotation and the specific allowable residual unbalance must be constant, i.e., to increase the speed of rotation it is necessary to reduce the specific residual unbalance.
This product is called Balance Quality Grade and it is designated by the letter G, see Table 1. To find a wide variety of existing rotors it was necessary to assign, depending on the type of rotor and its application, a value for this constant, see Table 1. Table 1 reproduces the G values which deals with quality of balancing rotating rigid bodies (ISO 1940-1, 2003).

3.3 Determination of unbalanced forces

As mentioned before, the unbalance of the rotor produces a dynamic load that depends on the mass, the equipment angular velocity and the eccentricity between the equipment

G	e x ω (mm/s)	Rotor Types - General Examples
G 4000	4000	Crankshaft/drives of rigidly mounted slow marine diesel engines with uneven number of cylinders.
G 1600	1600	Crankshaft/drives of rigidly mounted large two-cycle engines.
G 630	630	Crankshaft/drives of rigidly mounted large four-cycle engines; Crankshaft/drives of elastically mounted marine diesel engines.
G 250	250	Crankshaft/drives of rigidly mounted fast four-cylinder diesel engines.
G 100	100	Crankshaft/drives of fast diesel engines with six or more cylinders; Complete engines (gasoline or diesel) for cars, trucks and locomotives.
G 40	40	Car wheels, wheel rims, wheel sets, drive shafts; Crankshaft/drives of elastically mounted fast four-cycle engines with six or more cylinders; Crankshaft/drives of engines of cars, trucks and locomotives.
G 16	16	Drive shafts (propeller shafts, cardan shafts) with special requirements and parts of crushing machines; Individual components of engines (gasoline or diesel) for cars, trucks and locomotives; Crankshaft/drives of engines with six or more cylinders under special requirements.
G 6.3	6.3	Parts of process plant machines; Marine main turbine gears (merchant service); Centrifuge drums; Paper machinery rolls; print rolls; Fans; Assembled aircraft gas turbine rotors; Flywheels; Pump impellers; Machine-tool and general machinery parts; Medium and large electric armatures (electric motors having at least 80 mm shaft height) without special requirements; Small electric armatures, often mass produced, in vibration insensitive applications and/or with vibration-isolating mountings; Individual components of engines under special requirements.
G 2.5	2.5	Gas and steam turbines, including marine main turbines (merchant service); Rigid turbo-generator rotors; Computer memory drums and discs; Turbo-compressors; Machine-tool drives; Medium and large electric armatures with special requirements; Small electric armatures not qualifying for one or both of the conditions specified for small electric armatures of balance quality grade G 6.3; Turbine-driven pumps.
G 1	1	Tape recorder and phonograph (gramophone) drives; Grinding-machine drives; Small electric armatures with special requirements.
G 0.4	0.1	Spindles, discs and armatures of precision grinders; Gyroscopes.

Table 1. Balance quality values (ISO 1940-1, 2003)

gravity center and the rotation axis. In sequence, Equation (6) determines the dynamic load amplitude generated by the unbalance of a rotor, as follows:

$$P_0 = m \cdot R \cdot \Omega^2 = m \cdot (R\Omega) \cdot \Omega \tag{6}$$

Where:
P_0 : dynamic loading amplitude;
M : total mass in rotation;
Ω : equipment frequency;
R. Ω = G : equipment balance quality grade, see Table 1: (ISO 1940-1, 2003).
For rotors of electric motors, R.Ω was considered equal to 0.0025 m/s. Substituting this value in Equation (6), it is obtained:

$$P_0 = m \cdot (0.0025) \cdot \Omega \tag{7}$$

Considering an unbalanced load spinning around an axis, the procedure for obtaining the global dynamic force acting on a plane is to apply the force in two orthogonal directions. One of these forces is applied in the horizontal direction with the angle phase ϕ equal to zero and the other in vertical direction with the angle phase ϕ equal to 1/4 of the period of vibration of unbalanced force.
Thus, as time increases, there is a variation of the two forces so that the composition (horizontal and vertical directions) results in a harmonic unbalanced force where one component will be multiplied by sin (Ωt) and the other by sin (Ωt + π/2). This way, when one harmonic component presents maximum values the other one is equal to zero and vice versa. The value of the dynamic force is obtained by the vector sum of the components in the vertical and horizontal directions as presented in Equation (8).

$$P(t) = P_0 \sin(\Omega t) + P_0 \sin(\Omega t + \frac{\pi}{2}) \tag{8}$$

3.3 Dynamic loading modelling

To perform the numerical analysis of the oil production platform developed in this investigation, it was used the data in accordance with Table 2. In sequence, Figure 2 shows the design of the equipment.

Equipment data	
Protective cover	1.2 kN
Coupling	5.3 kN
Gear unit	37.5 kN
Motor swing	15 kN
Rotor weight	10.8 kN
Input frequency	30 Hz
Output frequency	0.94 Hz

Table 2. Equipment data

The dynamic load modelling considered two components related to vertical and horizontal directions. Table 3 shows the dynamic loads applied on the structural system steel deck. These actions were properly combined in order to better represent the dynamic excitation induced by equipment on the structure.

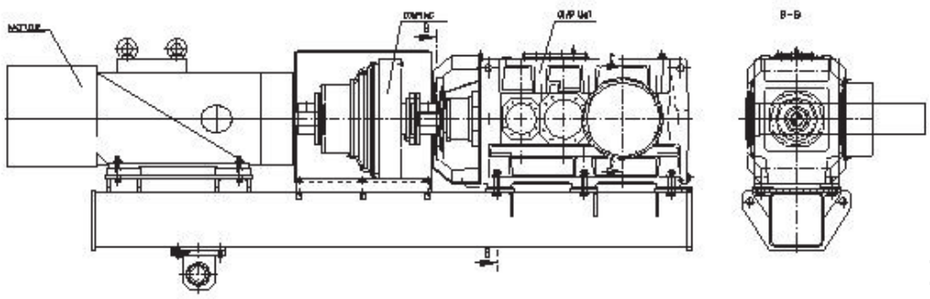

Fig. 2. Driving unit (motor, coupling and gear) supported by a steel beam (Rimola, 2010)

Equipment	Weight (kN)	Frequency (rad/s)	Rω (m/s)	P_0 (kN)
Rotor	10.80	188.49	0.0025	0.51
Gear	18.75	6.03	0.0025	0.028

Table 3. Dynamic actions related to the equipment

4. Investigated structural model

The structural system investigated in this paper is related to an oil production platform made of steel and located in Santos basin, São Paulo, Brazil. The structural model is supported by vertical sections made of tubular steel members (steel jacket), piled into the seabed by steel piles and consists of two steel decks with a total area of 1915 m² (upper deck: 445 m² and lower deck: 1470 m²), see Figures 3 and 4.

Fig. 3. Investigated structural model

The structural model is formed by steel beams and columns and steel deck plates, as presented in Figures 3 and 4. This platform is constituted by a lot of structural elements with very different geometrical characteristics; see (Rimola, 2010). A 2.05x105MPa Young's modulus was adopted for the steel beams, columns and decks.

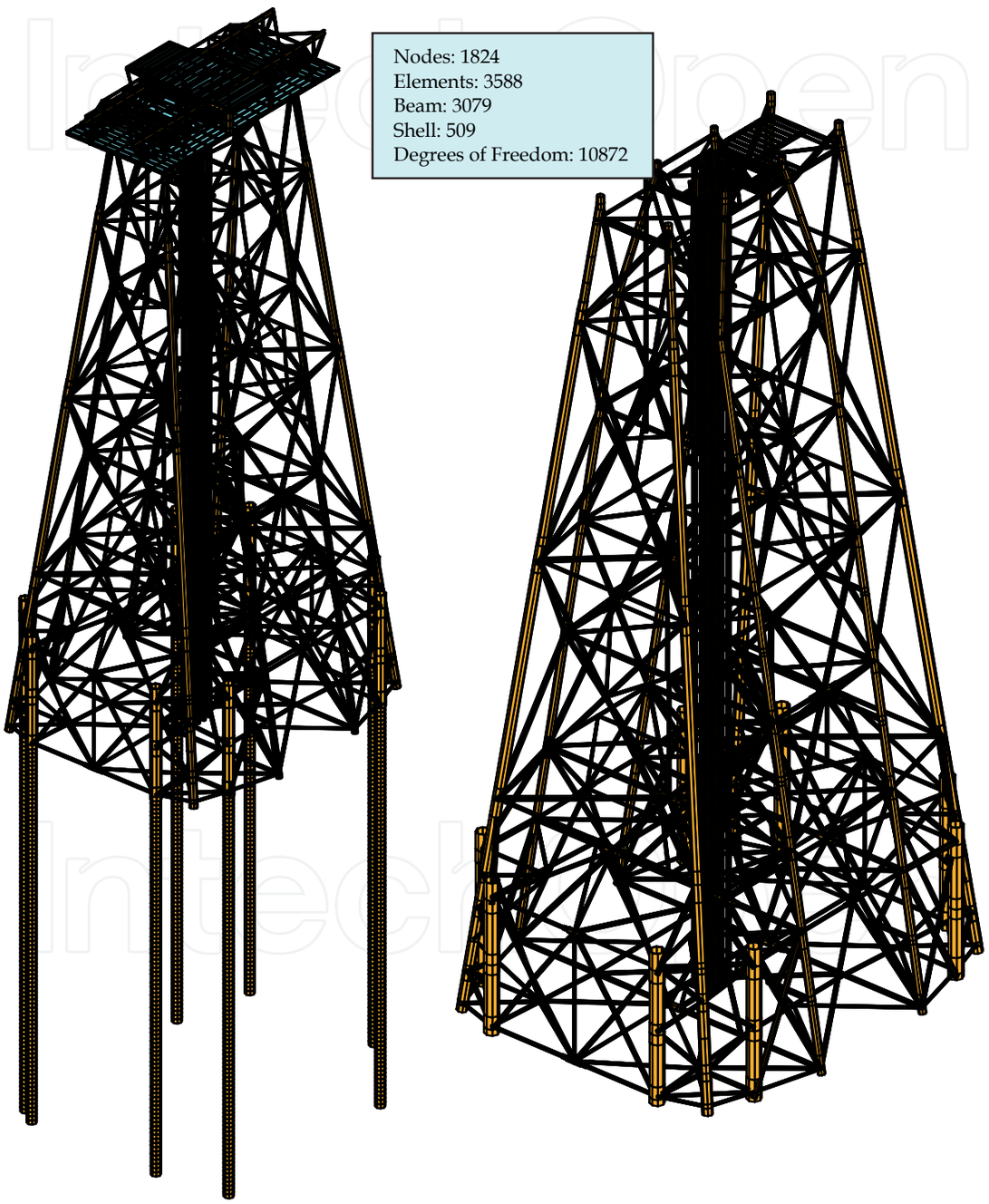

Fig. 4. Finite element model: oil production platform with steel jacket and piles

DEPTH	LAYERS DESCRIPTION	RESISTANCE PARAMETERS
6,090 ↓	Medium Sand	$\gamma_{sub} = 9{,}0\ kN/m^3$ $\phi = 30°$
18,280 ↓	Stiff Clay	$\gamma_{sub} = 8{,}0\ kN/m^3$ $C = 70{,}75 kN/m^2$
21,940 ↓	Fine Sand	$\gamma_{sub} = 8{,}9\ kN/m^3$ $\phi = 30°$
24,990 ↓	Medium Clay	$\gamma_{sub} = 8{,}0\ kN/m^3$ $C = 80{,}90 kN/m^2$
34,130 ↓	Medium Sand	$\gamma_{sub} = 8{,}9\ kN/m^3$ $\phi = 35°$
42,970 ↓	Fine Sand	$\gamma_{sub} = 8{,}9\ kN/m^3$ $\phi = 25°$
54,860 ↓	Stiff Clay	$\gamma_{sub} = 8{,}0\ kN/m^3$ $C = 113{,}55 kN/m^2$
67,050 ↓	Stiff Clay	$\gamma_{sub} = 8{,}0\ kN/m^3$ $C = 138{,}75 kN/m^2$
79,240 ↓	Stiff Clay	$\gamma_{sub} = 8{,}0\ kN/m^3$ $C = 164{,}20 kN/m^2$
103,00 ↓	Stiff Clay	$\gamma_{sub} = 8{,}0\ kN/m^3$ $C = 192{,}05 kN/m^2$

Fig. 5. Geotechnical profile

5. Computational modelling

The proposed computational model, developed for the structural system dynamic analysis, adopted the usual mesh refinement techniques present in finite element method simulations implemented in the GTSTRUDL program (GTSTRUDL, 2009).

In this computational model, floor steel girders and columns were represented by a three-dimensional beam element with tension, compression, torsion and bending capabilities. The element has six degrees of freedom at each node: translations in the nodal x, y, and z directions and rotations about x, y, and z axes. On the other hand, the steel deck plates were represented by shell finite elements (GTSTRUDL, 2009).
In this investigation, it was considered that both structural elements (steel beams and steel deck plates) have total interaction with an elastic behaviour. The finite element model has 1824 nodes, 3079 three-dimensional beam elements, 509 shell elements and 10872 degrees of freedom, as presented in Figure 4.

5.1 Geotechnical data

The data related to soil were obtained by means of three boreholes (Standard Penetration Tests: SPT) in a depth range varying from 43.5m to 178.3m. The boreholes allowed the definition of the geotechnical profile (Figueiredo Ferraz, 2004) adopted in the finite element modelling, see Figure 5. Characterisation and resistance tests performed in laboratory provided specific weight, friction angle and cohesion values illustrated in Figure 5. In Figure 5, γ_{sub} is the submerged specific weight (kN/m^3); c represents the soil cohesion in (kN/m^2) and ϕ is soil friction angle (degree).

5.2 Soil-structure interaction

When the study of half-buried columns is considered, the usual methodology to the formulation of the soil-structure interaction problem utilizes the reaction coefficient concept, originally proposed by (Winkler, 1867). In the case of laterally loaded piles, the analysis procedure based on (Winkler, 1867) is analogue to the one used for shallow foundations, see Figure 6.
The soil behaviour is simulated by a group of independent springs, governed by a linear-elastic model. The foundation applies a reaction in the column normal direction and it is proportional to the column deflection. The spring stiffness, designated by reaction coefficient (k_h) is defined as the necessary pressure to produce a unitary displacement (Winkler, 1867), as presented in Equation (9).

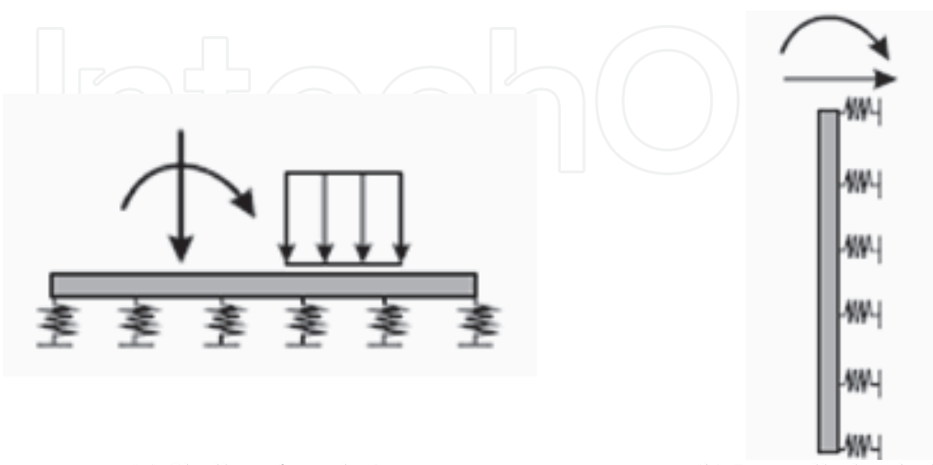

(a) Shallow foundation (b) Laterally loaded pile

Fig. 6. Foundation analysis models

$$k_h = \frac{p}{y} \tag{9}$$

Where:
p : applied pressure, in (N/m²);
y : soil deflection, in (m).
(Terzaghi, 1955) considered that the reaction coefficient (k_h) for piles in cohesive soils (clays), does not depend on the depth of the pile and may be determined by the following equation.

$$k_h = \frac{0.3048\,m}{1.5\,d} \times (k_{s1}) \tag{10}$$

Where:
k_{s1} : modulus to a squared plate with a length of 0.3048m (1 ft), in (MN/m³);
d : column width (pile), in (m).
Table 4 presents typical values for k_{s1} for consolidated clays.

Clay's consistency	k_{s1} (t/ft³)	k_{s1} (MN/m³)
Stiff	75	26.0
Very Stiff	150	52.0
Hard	300	104.0

Table 4. Typical values for k_{s1} (Terzaghi, 1955)

For piles in non-cohesive soils (sand), it is considered that the horizontal reaction coefficient (k_h) varies along the depth, according to Equation (11).

$$k_h = n_h \frac{z}{d} \tag{11}$$

Where:
n_h : stiffness parameter for non-cohesive soils, in (MN/m³);
d : column width (pile), in (m).
Typical values for n_h obtained by (Terzaghi, 1955), as a function of the sand relative density under submerged and dry condition, are presented in Table 5.

Relative density	n_h (dry) (t/ft³)	n_h (dry) (MN/m³)	n_h (submerged) (t/ft³)	n_h (submerged) (MN/m³)
Loose	7	2.4	4	1.4
Medium	21	7.3	14	4.9
Dense	56	19.4	34	11.8

Table 5. Typical values for n_h (Terzaghi, 1955)

Based on the horizontal reaction coefficients values (k_h) and the column width (d), the foundation stiffness parameter (k_0) is determined by using Equation (12) (Poulos & Davis, 1980):

$$k_0 = k_h \times d \tag{12}$$

Based on the subsoil geotechnical profile (see Figure 5) and using the analysis procedure based on the Winkler model (Winkler, 1867) the horizontal reaction coefficients on the piles (k_h) were determined as a function of the type of the soil. Applying the horizontal reaction coefficients (k_h) on Equation (12), the foundation stiffness parameters values (k_0) were calculated.

The foundation stiffness parameters values (k_0) were used to determine the spring's stiffness (k) placed in the computational model to simulate the soil behaviour. The spring elements which simulate the piles were discretized based on a range with length equal to 1m (one meter). For each range of 1m it was placed a translational spring in the transversal direction of the pile section axis with a stiffness value equal to the value obtained for the horizontal reaction coefficient evaluated by the Winkler model (Winkler, 1867). Table 6 presents the spring's stiffness coefficients simulating.

Depth (m)	Layer Description	Pile Profile		Spring's stiffness k (kN/m)
		Ø (mm)	Thickness (mm)	
1	Medium sand	2108	55	4850.1163
2				9700.2327
3				14550.3490
4				19400.4653
5				24250.5816
6				29100.6980
7 a 18	Stiff clay	2134	55	5279.6981
19	Fine sand	2134	55	92152.2102
20				97002.3266
21				101852.4429
22				106702.5592
23 a 25	Medium clay	2134	55	281.5839
26	Medium sand	2134	55	126103.0245
27				130953.1408
28				135803.2572
29				140653.3735
30				145503.4898
31				150353.6062
32				155203.7225
33				160053.8388
34				164903.9551
35	Fine sand	2134	55	169754.0715
36				174604.1878
37				179454.3041
38				184304.4204
39				189154.5368
40				194004.6531
41				198854.7694
42				203704.8858
43				208555.0021
44 a 96	Stiff clay	2134	55	5279.6981

Table 6. Stiffness coefficients of soil representative springs

5.3 Structural damping modelling

It is called damping the process which energy due to structural system vibration is dissipated. However, the assessment of structural damping is a complex task that cannot be determined by the structure geometry, structural elements dimensions and material damping (Clough & Penzien, 1995).

According to (Chopra, 2007), it is impossible to determine the damping matrix of a structural system through the damping properties of each element forming the structure with the same way it is determined the structure stiffness matrix, for example. This is because unlike the elastic modulus, which is used in the stiffness evaluation, the damping materials properties are not well established.

Although these properties were known (Chopra, 2007), the resulting damping matrix would not take into account a significant portion of energy dissipated by friction in the structural steel connections, opening and closing micro cracks in the concrete, friction between structure and other elements that are bound to it, such as masonry, partitions, mechanical equipment, fire protection, etc. Some of these energy dissipation sources are extremely difficult to identify.

The physical evaluation of the damping of a structure is not considered properly as if their values are obtained by experimental tests. However, these tests often require time and cost that in most cases is very high. For this reason, damping is usually achieved in terms of contribution rates, or rates of modal damping (Clough & Penzien, 1995).

With this in mind, it is common to use the Rayleigh damping matrix, which considers two main parts, one based on the mass matrix contribution rate (α) and another on the stiffness matrix contribution rate (β), as can be obtained using Equation (13). It is defined **M** as the mass matrix and **K** as the stiffness matrix of the system (Craig Jr., 1981; Clough & Penzien, 1995; Chopra, 2007).

$$\mathbf{C} = \alpha\mathbf{M} + \beta\mathbf{K} \tag{13}$$

Equation (13) may be rewritten, in terms of the damping ratio and the circular natural frequency (rad/s), as presented in Equation (14):

$$\xi_i = \frac{\alpha}{2\omega_{0i}} + \frac{\beta\omega_{0i}}{2} \tag{14}$$

Where:

ξ_i : damping ratio related to the i^{th} vibration mode;

ω_{0i} : circular natural frequency related to the i^{th} vibration mode.

Isolating the coefficients α and β from Equation (14) and considering the two most important structural system natural frequencies, Equations (15) and (16) can be written.

$$\alpha = 2\xi_i\omega_{01} - \beta\omega_{01}\omega_{01} \tag{15}$$

$$\beta = \frac{2\left(\xi_2\omega_{02} - \xi_1\omega_{01}\right)}{\omega_{02}\omega_{02} - \omega_{01}\omega_{01}} \tag{16}$$

Based on two most important structural system natural frequencies it is possible to calculate the values of α and β. In general, the natural frequency ω_{01} is taken as the lowest natural

frequency, or the structure fundamental frequency and ω_{02} frequency as the second most important natural frequency.

In the technical literature, there are several values and data about structural damping. In fact, these values appear with great variability, which makes their use in structural design very difficult, especially when some degree of systematization is required. Based on the wide variety of ways to considering the structural damping in finite element analysis, which, if used incorrectly, provide results that do not correspond to a real situation, the design code CEB 209/91 (CEB 209/91, 1991) presents typical rates for viscous damping related to machinery support of industrial buildings, as shown in Table 7.

Construction Type	Minimum	Mean	Maximum
Reinforced Concrete	0.010	0.017	0.025
Prestressed Concrete	0.007	0.013	0.020
Composite Structures	0.004	0.007	0.012
Steel	0.003	0.005	0.008

Table 7. Typical values of damping ratio ξ for industrial buildings (CEB 209/91, 1991)

Based on these data, it was used a damping coefficient of 0.5% (ξ = 0.5% or 0.005) in all modes. This rate takes into account the existence of few elements in the oil production platform that contribute to the structural damping. Table 8 presents the parameters α and β used in the forced vibration analysis to model the structural damping in this investigation.

f_{01} (Hz)	f_{02} (Hz)	ω_{01} (rad/s)	ω_{02} (rad/s)	α	β
0.674	0.716	4.2364	4.4968	0.02172	0.00115

Table 8. Values of the coefficients α and β values used in forced vibration analysis

6. Natural frequencies and vibration modes

The production platform natural frequencies were determined with the aid of the numerical simulations, see Table 9, and the corresponding vibration modes are shown in Figure 7 and 8. Each natural frequency has an associated mode shape and it was observed that the first vibration modes presented predominance of the steel jacket system.

Natural Frequencies f_{0i} (Hz)		Vibration Modes	
f_{01}	0.67	Mode 1	Vibration modes with predominance of the steel jacket system.
f_{02}	0.71	Mode 2	
f_{03}	1.20	Mode 3	
f_{08}	1.99	Mode 8	Vibration modes with predominance of the steel deck displacements.
f_{17}	2.61	Mode 17	
f_{49}	4.14	Mode 49	

Table 9. Production platform natural frequencies

It can be observed in Figure 7, that the three first vibration modes presented predominance of displacements in the steel jacket system. In the 1st vibration mode there is a predominance of translational displacements towards the "y" axis in the finite element model. In the 2nd vibration mode a predominance of translational effects towards the axis "x" of the numerical model was observed. The third vibration mode presented predominance of torsional effects on the steel jacket system with respect to vertical axis "z". Flexural effects were predominant on the steel deck system and can be seen only from higher order vibration modes, see Figure 8.

However, flexural effects were predominant in the steel deck plate (upper and lower), starting from the eighth vibration mode (f_8 = 1.99 Hz - Vibration Mode 8), see Table 9. It is important to emphasize that torsional effects were present starting from higher mode shapes, see Table 9. Figures 7 and 8 illustrated the mode shapes corresponding to six natural frequencies of the investigated structural system.

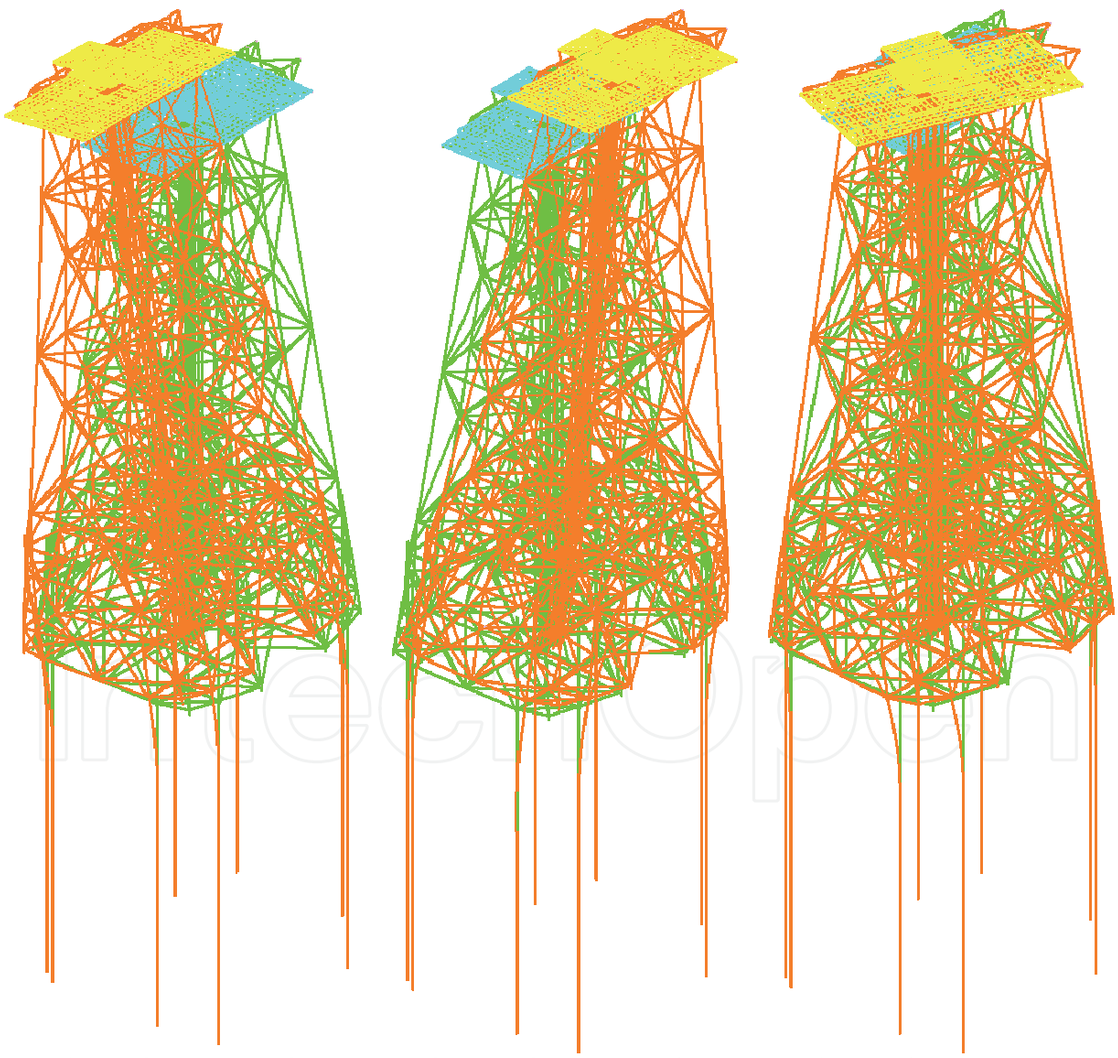

a) 1st vibration mode b) 2nd vibration mode c) 21st vibration mode

Fig. 7. Vibration modes with predominance of the steel jacket system

7. Structural system dynamic response

The present investigation proceeds with the evaluation of the steel platform's performance in terms of vibration serviceability effects, considering the impacts produced by mechanical equipment (rotating machinery). This strategy was considered due to the fact that unbalanced rotors generate vibrations which may damage their components and supports and produce dynamic actions that could induce the steel deck plate system to reach unacceptable vibration levels, leading to a violation of the current human comfort criteria for these specific structures. For this purpose, forced vibration analysis is performed through using the computational program (GTSTRUDL, 2009). The results of forced vibration models are obtained in terms of the structural system displacements, velocities and peak accelerations.

For the structural analysis, it was considered the simultaneous operation of three machines on the steel deck. The nodes of application of dynamic loads in this situation are shown in Figure 9. With respect to human comfort, some nodes of the finite element model were selected near to the equipment in order to evaluate the steel deck dynamic response (displacements, velocities and accelerations). These nodes are also shown in Figure 9.

The dynamic loading related to the rotor was applied on the nodes 9194, 9197 and 9224 and the corresponding dynamic loading associated to the gear was applied on the nodes 9193, 9196 and 9223, as presented in Figure 9. The description of the dynamic loadings (rotor and gear) was previously described on item 3. It should be noted that the positioning of the machines was based on the equipment arrangement drawings of the investigated platform (Figueiredo Ferraz, 2004).

The analysis results were compared with limit values from the point of view of the structure, operation of machinery and human comfort provided by international design recommendations (CEB 209/91, 1991; ISO 1940-1, 2003; ISO 2631-1, 1997; ISO 2631-2, 1989; Murray et al., 2003). It must be emphasized that only the structural system steady-state response was considered in this investigation.

The frequency integration interval used in numerical analysis was equal to 0.01 Hz ($\Delta\omega$ = 0.01 Hz). It was verified that the frequency integration interval simulated conveniently the dynamic characteristics of the structural system and also the representation of the proposed dynamic loading (Rimola, 2010).

In sequence of the study, Tables 10 to 12 present the vertical translational displacements, velocities and accelerations, related to specific locations on the steel deck, near to the mechanical equipment, see Figure 9, calculated when the combined dynamic loadings (rotor and gear) were considered.

These values, obtained numerically with the aid of the proposed computational model, were then compared with the limiting values proposed by design code recommendations (CEB 209/91, 1991; ISO 1940-1, 2003; ISO 2631-1, 1997; ISO 2631-2, 1989; Murray et al., 2003). Once again, it must be emphasized that only the structural system steady state response was considered in this investigation.

The allowable amplitudes are generally specified by manufactures of machinery. When manufacture's data doesn't indicate allowable amplitudes, design guides recommendations (ISO 1940-1, 2003) are used to determine these limiting values for machinery performance, see Table 10. The maximum amplitude value at the base of the driving support (Node 9197: see Figure 9), on the platform steel deck was equal to 446 μm (or 0.446 mm or 0.0446 cm), see Table 10, indicating that the recommended limit value was violated and the machinery performance can be inadequate (0.446 mm > 0.06 mm) (ISO 1940-1, 2003).

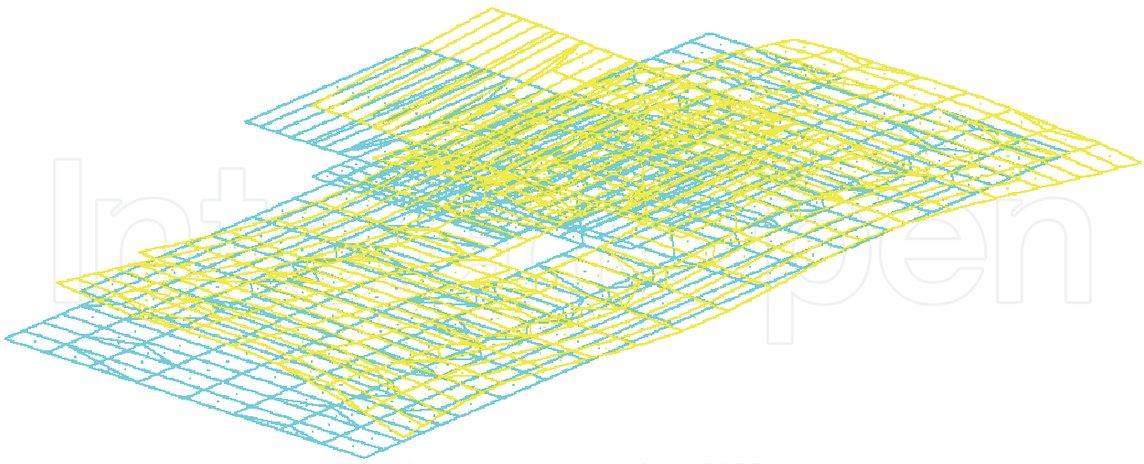

a) 8th vibration mode f_{08}=1.99 Hz

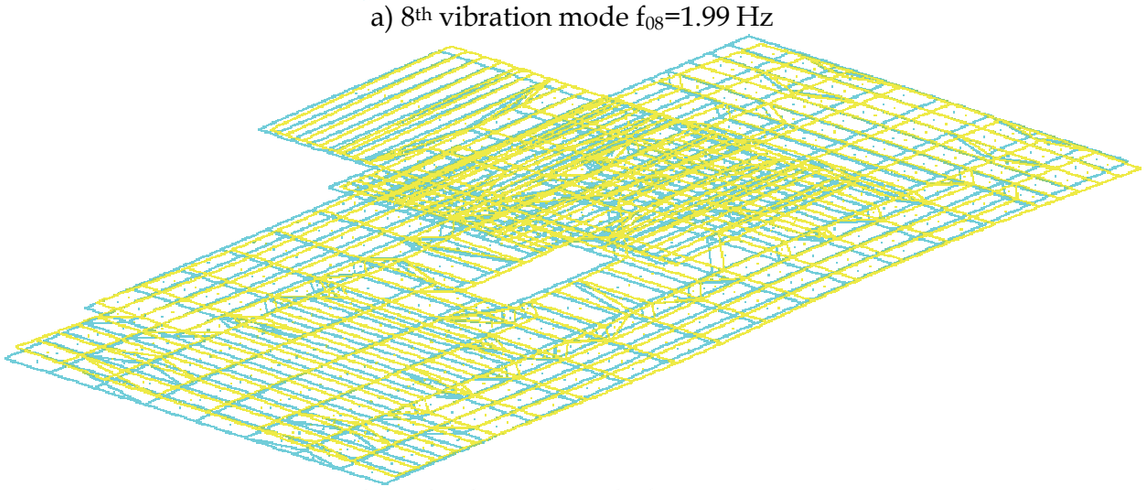

b) 17th vibration mode f_{17}=2.61 Hz

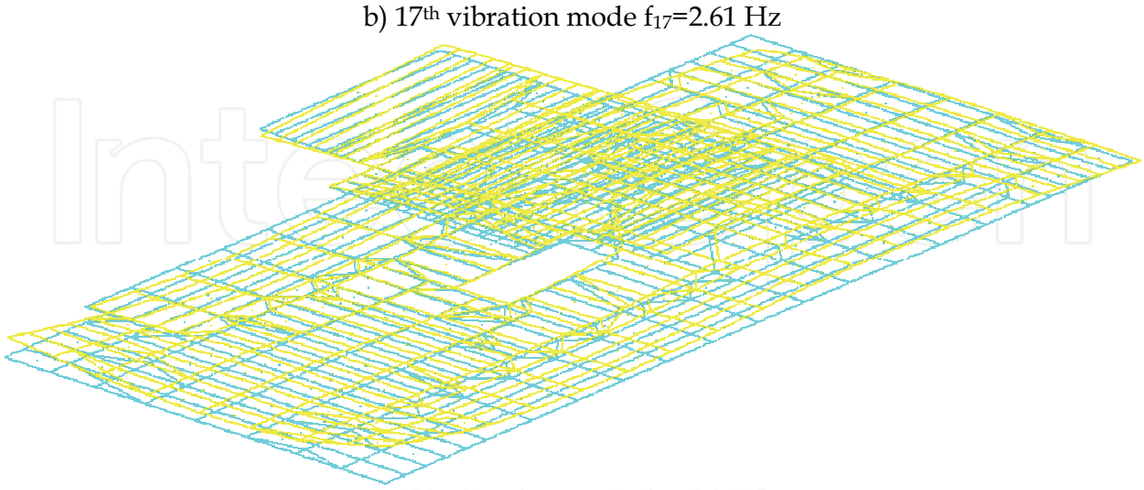

c) 49th vibration mode f_{49}=4.14 Hz

Fig. 8. Vibration modes with predominance of the steel deck system

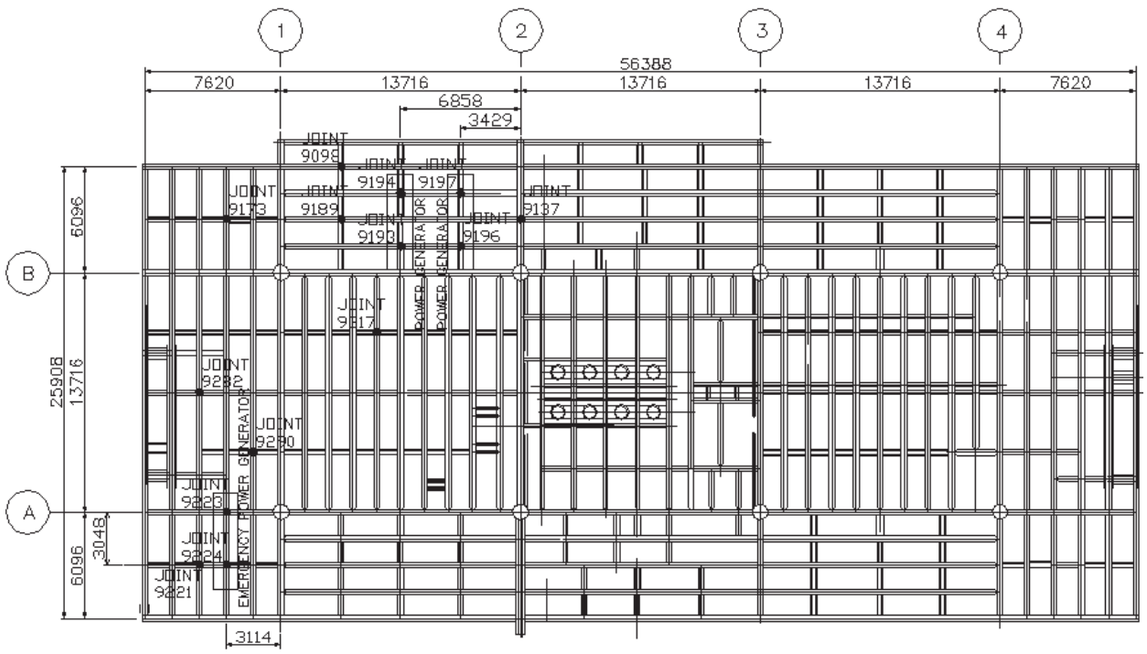

Fig. 9. Selected nodes for application of the dynamic loads

Rotor Support (Node: 9194) (μm)	Rotor Support (Node: 9197) (μm)	Rotor Support (Node: 9224) (μm)	Amplitude Limit Values (μm)
54	**446**	7	40 to 60*
Gear Support (Node: 9193) (μm)	Gear Support (Node: 9196) (μm)	Gear Support (Node: 9223) (μm)	
77	432	38	
* For vertical vibration for high speed machines (>1500 rpm) (ISO 1940-1, 2003).			

Table 10. Vertical displacements related to the combined dynamic loading (driving)

Rotor Support (Node: 9194) (mm/s)	Rotor Support (Node: 9197) (mm/s)	Rotor Support (Node: 9224) (mm/s)	Velocity Limit Values (mm/s)
10.18	**84.12**	11.89	0.70 to 2.80*
Gear Support (Node: 9193) (mm/s)	Gear Support (Node: 9196) (mm/s)	Gear Support (Node: 9223) (mm/s)	
14.49	81.46	7.27	
* Tolerable velocity for electrical motors according to (ISO 1940-1, 2003).			

Table 11. Velocities related to the combined dynamic loading (driving)

The maximum velocity value calculated at the base of the driving support (Node 9197: see Figure 9), on the platform steel deck was equal to 84.12 mm/s, see Table 11. The allowable velocity considering a perfect condition to machinery performance is located in the range of 0.7mm/s to 2.8 mm/s, see (ISO 1940-1, 2003), as presented in Table 11. This velocity value is

not in agreement with those proposed by the design codes (84.12 mm/s > 2.8 mm/s) (ISO 1940-1, 2003), violating the recommended limits.

Steel Deck (Node: 9098) (m/s^2)	Steel Deck (Node: 9137) (m/s^2)	Steel Deck (Node: 9173) (m/s^2)	Steel Deck (Node: 9189) (m/s^2)	Acceleration Limit Values (m/s^2)
5.62	6.16	4.67	**27.33**	0.315 to 1.0*
Steel Deck (Node: 9221) (m/s^2)	Steel Deck (Node: 9282) (m/s^2)	Steel Deck (Node: 9290) (m/s^2)	Steel Deck (Node: 9317) (m/s^2)	
11.62	8.19	11.77	0.61	
* Acceptable acceleration values for human comfort in accordance with (ISO 2631-1, 1997).				

Table 12. Accelerations related to the combined dynamic loading (driving)

People working temporarily near to driving could be affected in various degrees (human discomfort). The allowable acceleration value when the human comfort is considered (ISO 2631-1, 1997) is located in the range of 0.315 m/s^2 to 1.0 m/s^2, as illustrated in Table 12. The peak acceleration value calculated on the platform steel deck was equal to 27.33 m/s^2, see Table 12. This maximum acceleration value violated the recommended limits proposed by the design codes (27.33 m/s^2 > 1.0 m/s^2) (ISO 2631-1, 1997), causing human discomfort.

Based on the numerical results obtained with the present investigation, it was clearly demonstrated that the investigated structural model presented problems due to excessive vibration. This way, some changes on the horizontal steel bracing system were proposed by the authors, in order to reduce the vibration effects.

This way, Figure 10 shows the proposed steel bracing members which were added to the original design of the investigated structural model. The central idea was to propose a bracing system that produces an increasing in the steel deck stiffness and, consequently, can cause a reduction of the steel deck system dynamic response, when submitted to the rotor and gear dynamic loads.

In sequence, Figure 11 shows the vibration modes of the production platform steel deck system before and after the addition of the proposed bracing members shown in Figure 10. Comparing the presented vibration modes, it may be concluded that modal amplitudes have been modified, leading to a reduction of the structural system dynamic response, in terms of displacements, velocities and accelerations.

Figure 12 shows the response spectra of vertical translational displacements, for the supports and rotors, and, for particular nodes of the steel deck of the platform. Only three graphs were presented due to the fact that this figure (Figure 12) represents, in general, the dynamic response of the system. Based on the structure dynamic response, the peak of interest for the forced vibration numerical analysis, associated with the excitation frequency of the equipment (f = 30 Hz) is indicated in the Figure 12.

Tables 13 to 15 present the vertical translational displacements, velocities and accelerations, related to specific locations on the steel deck, near of the mechanical equipment, see Figure 9, calculated with the introduction of the proposed steel bracing system, when the combined dynamic loadings were considered.

The values presented in Tables 13 to 15 were obtained numerically with the aid of the developed finite element model. These values were then compared with the limiting values proposed by design code recommendations (CEB 209/91, 1991; ISO 1940-1, 2003; ISO 2631-1,

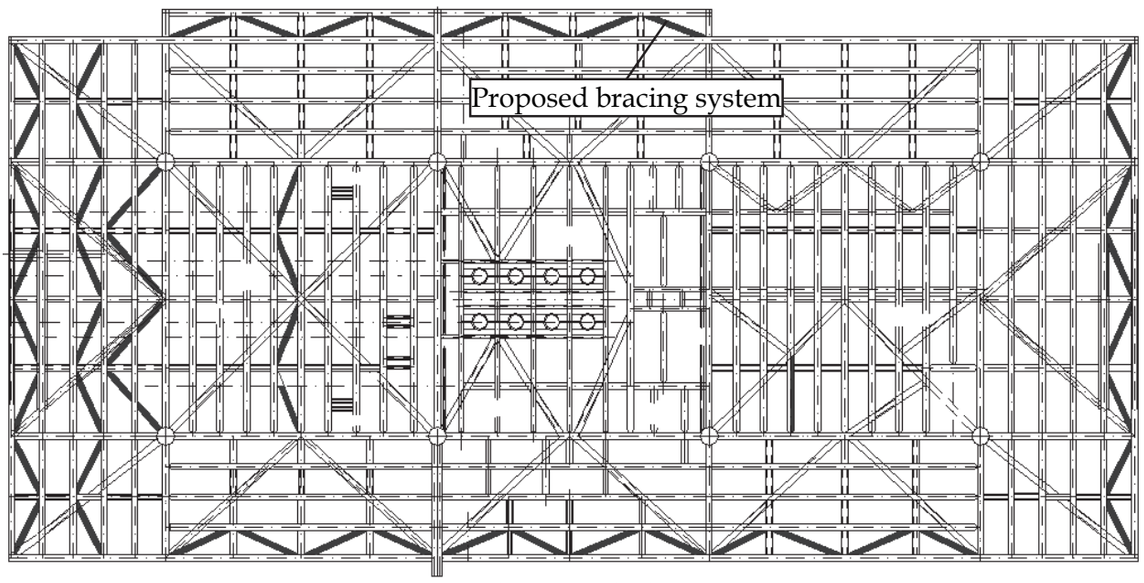

a) Lower deck

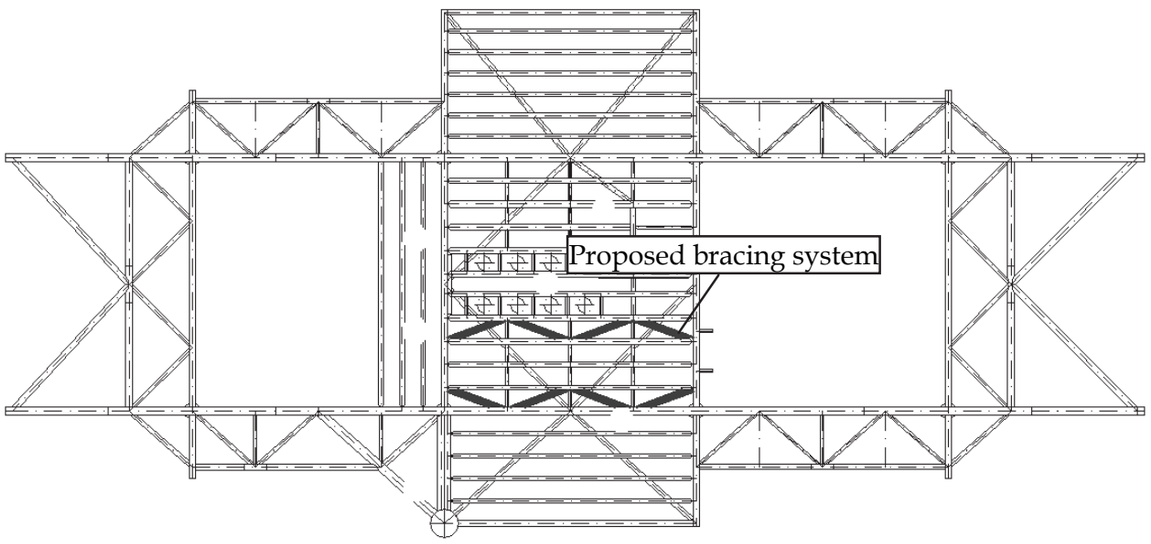

b) Upper deck

Fig. 10. Steel deck with the introduction of the proposed bracing system

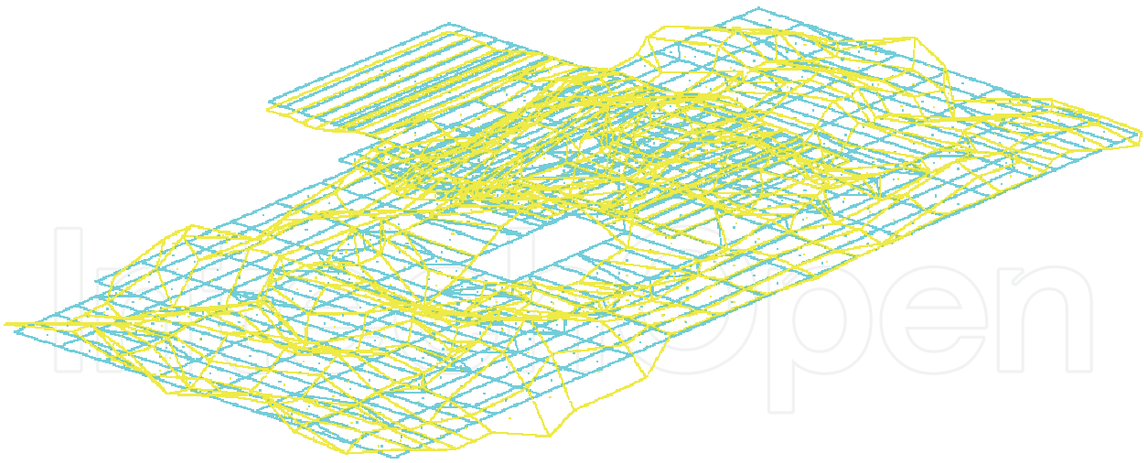

a) Before the introduction of the bracing system. Mode: 1203 - Frequency: 30 Hz

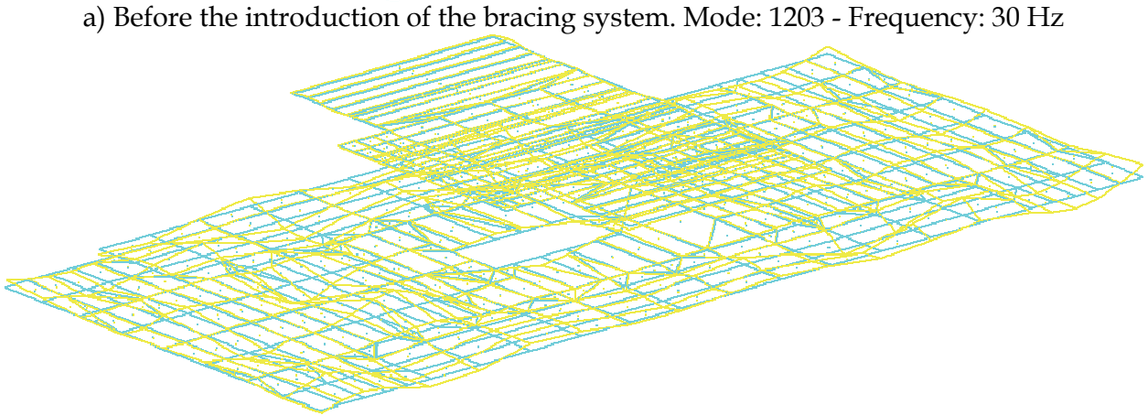

b) After the introduction of the bracing system. Mode: 1195 - Frequency: 30 Hz

Fig. 11. Steel deck vibration modes

1997; ISO 2631-2, 1989; Murray et al., 2003), after the introduction of the proposed bracing system. It must be emphasized, that only the production platform steady state response was considered in this analysis.

Considering the Figure 12 (12a, 12c and 12e), related to the production platform steel deck dynamic response, it can be verified the existence of several energy transfer areas with several energy transfer picks, before the addition of the proposed bracing system.

The peak of interest for the forced vibration numerical analysis, associated with the excitation frequency of the equipment (f = 30 Hz) is clearly indicated in this figure, see Figure 12 (12a, 12c and 12e). However, after the introduction of the proposed bracing system, the energy transfer pick related to the excitation frequency of the equipment was significantly reduced, see Figure 12 (12b, 12d and 12f). This fact demonstrates the efficiency of the proposed bracing system and indicates that the structural system dynamic response can be significantly reduced.

Considering the same strategy previously presented, the design recommendations (see Tables 10 to 12) were utilized, in order to determine the limiting values for machinery performance, related to allowable amplitudes, velocities and accelerations (ISO 1940-1, 2003; ISO 2631-1, 1997).

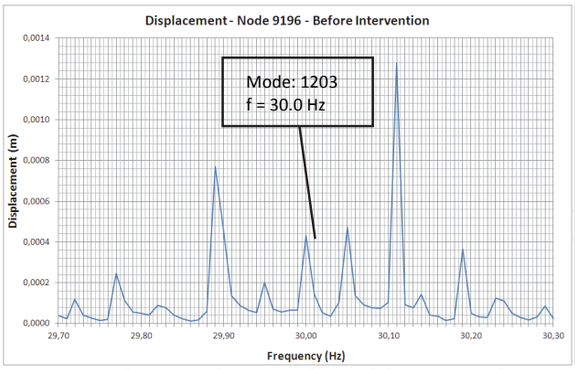

a) Node 9196 before the addition of the bracing system

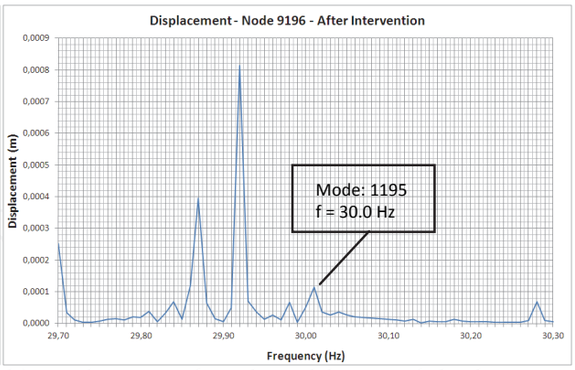

b) Node 9196 after the addition of the bracing system

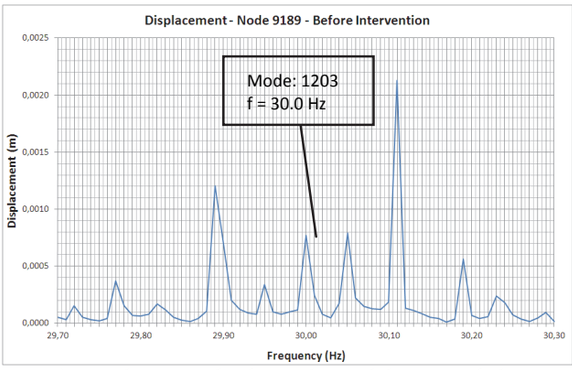

c) Node 9189 before the addition of the bracing system

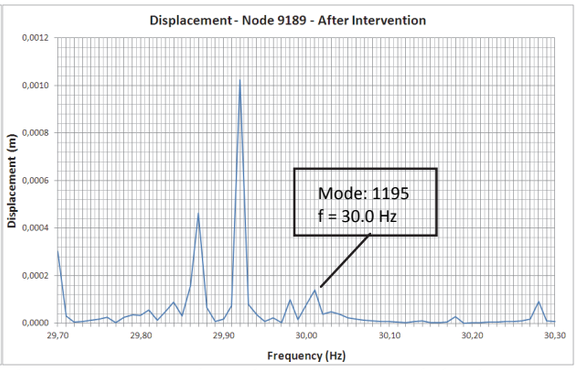

d) Node 9189 after the addition of the bracing system

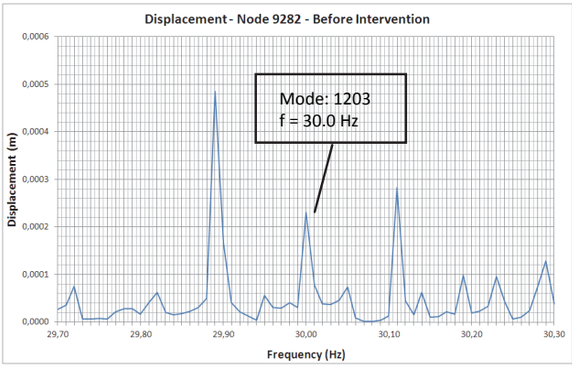

e) Node 9282 before the addition of the bracing system

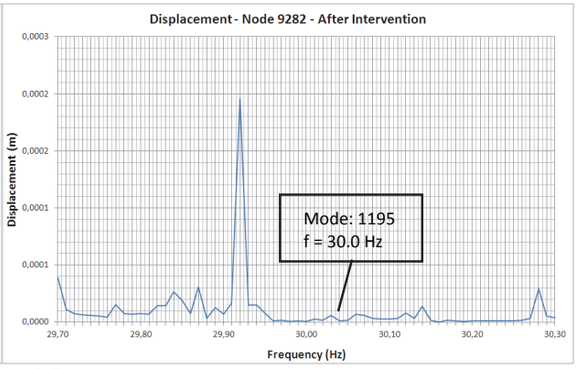

f) Node 9282 after the addition of the bracing system

Fig. 12. Vertical displacements response spectra of the steel deck selected joints before and after the introduction of the proposed bracing system

Rotor Support (Node: 9194) (μm)	Rotor Support (Node: 9197) (μm)	Rotor Support (Node: 9224) (μm)	Amplitudes Limit Value (μm)
35	**96**	54	40 to 60*
Gear Support (Node: 9193) (μm)	Gear Support (Node: 9196) (μm)	Gear Support (Node: 9223) (μm)	
33	52	5	
* For vertical vibration for high speed machines (>1500 rpm) (ISO 1940-1, 2003).			

Table 13. Vertical displacements related to the combined dynamic loading (driving), after the addition of the proposed bracing system

Rotor Support (Node: 9194) (mm/s)	Rotor Support (Node: 9197) (mm/s)	Rotor Support (Node: 9224) (mm/s)	Velocities Limit Value (mm/s)
6.68	6.92	**10.36**	0.70 to 2.80*
Gear Support (Node: 9193) (mm/s)	Gear Support (Node: 9196) (mm/s)	Gear Support (Node: 9223) (mm/s)	
6.23	9.80	2.71	
* Tolerable velocity for electrical motors according to (ISO 1940-1, 2003).			

Table 14. Velocities related to the combined dynamic loading (driving), after the addition of the proposed bracing system

Steel Deck (Node: 9098) (m/s^2)	Steel Deck (Node: 9137) (m/s^2)	Steel Deck (Node: 9173) (m/s^2)	Steel Deck (Node: 9189) (m/s^2)	Amplitudes Limit Value (m/s^2)
1.39	0.50	2.63	**4.96**	0.315 to 1.0*
Steel Deck (Node: 9221) (m/s^2)	Steel Deck (Node: 9282) (m/s^2)	Steel Deck (Node: 9290) (m/s^2)	Steel Deck (Node: 9317) (m/s^2)	
3.44	0.20	1.23	2.75	
* Acceptable acceleration values for human comfort in accordance with (ISO 2631-1, 1997).				

Table 15. Accelerations related to the combined dynamic loading (driving), after the addition of the proposed bracing system

This way, after the addition of the bracing system, see Figure 10, the structural system dynamic response, submitted to the dynamic loadings (driving) coming from the machinery presented the following results: the maximum amplitude value at the base of the driving support (Node 9197: see Figure 9) on the platform steel deck was reduced of 446 μm (or 0.446 mm or 0.0446 cm) to 96 μm (or 0.096 mm or 0.0096 cm), see Tables 10 and 13; the maximum velocity value calculated at the base of the driving support (Node 9197: see Figure 9), on the steel deck was reduced of 84.12 mm/s to 6.92 mm/s, see Tables 11 and 14; the peak acceleration value calculated on the structure steel deck was reduced of 27.33 m/s² to 4.96 m/s², see Tables 12 and 15.
It must be emphasized that despite the fact that the limiting values for machinery performance, related to allowable amplitudes, velocities and accelerations (ISO 1940-1, 2003; ISO 2631-1, 1997) were violated, even after the addition of the proposed bracing system, the steady-state structural system dynamic response was considerably reduced.

8. Final remarks

This paper investigated the dynamic behaviour of an oil production platform made of steel and located in Santos basin, São Paulo, Brazil. The structural model consists of two steel decks with a total area of 1915 m² (upper deck: 445 m² and lower deck: 1470 m²), supported by vertical sections made of tubular steel members (steel jacket), and piled into the seabed, when subjected to impacts produced by mechanical equipment (rotating machinery). The main objective of the paper was to assess the dynamic impacts on the steel deck structure coming from the electrical generators and compressors.
Based on the peak acceleration values and maximum displacements and velocities, obtained on the structure steady-state response, it was possible to evaluate the structural model performance in terms of human comfort, maximum tolerances of the mechanical equipment and vibration serviceability limit states of the structural system, based on the design code recommendations.
It was concluded that the oil production platform displacements response spectra presented several energy transfer areas with several energy transfer picks. However, after the introduction of the horizontal steel bracing system proposed by the authors, the energy transfer pick related to the excitation frequency of the equipment was significantly reduced, demonstrating the efficiency of the idealized system.
After the addition of the horizontal bracing system the structural system dynamic response presented the following results: the maximum amplitude value at the base of the driving support on the steel deck was reduced of 0.0446 cm to 0.0096 cm; the maximum velocity value calculated at the base of the driving support on the deck was reduced of 84.12 mm/s to 6.92 mm/s and the maximum acceleration value calculated on the structure steel deck was reduced of 27.33 m/s² to 4.96 m/s².
However, even considering the improvement on the structural model bracing system and a considerably reduction on the structure dynamic response, the results obtained throughout this investigation indicated that the analysed platform steel deck violated the human comfort criteria, as well as its vibration serviceability limit states, inducing that individuals working temporarily near the machinery could be affected by human discomfort.

On the other hand, considering the machinery performance, it was also concluded that the platform steel deck design, should be revaluated, due to the fact that the displacements and velocities values related to the machinery supports were very high and violated the recommended limits proposed by design codes.

9. Acknowledgements

The authors gratefully acknowledge the support for this work provided by the Brazilian Science Foundations: CAPES, CNPq and FAPERJ.

10. References

Assunção, T. M. R. C. (2009). "*Considerações sobre efeitos dinâmicos e carregamentos induzidos por fontes de excitação em estruturas*". MSc Dissertation (In Portuguese), Civil Engineering Post-graduate Programme, Federal University of Minas Gerais, UFMG, Minas Gerais, MG, Brazil.

Bachmann, H.; Ammann, W. (1987). *Vibrations in Structures: Induced by Man and Machines*, Structural Engineering Document 3rd Ed., International Association for Bridges and Structural Engineering.

Chopra, A. K. (2007). *Dynamics of Structures – Theory and Applications to Earthquake Engineering*. 3rd Ed., Pearson Education, Inc., New Jersey.

Clough, R. W.; Penzien, J. (1995). *Dynamics of Structures*, 3rd Ed., Computers and Structures, Inc., Berkeley.

Comité Euro-International Du Beton. (1991). *Vibration Problems in Structures - Practical Guidelines*. Bullitin dínformation nº 209.

Craig JR., R. R. (1981). *Structural Dynamics – An Introduction to Computer Methods*. John Wiley& Sons, Inc., New York.

Dias Junior, M. "Dinâmica de Rotores". Proceedings of IV Congresso da Academia Trinacional de Ciências, Paraná, PR, Brazil, October 2009, Fozdo Iguaçu.

Figueiredo Ferraz Consultoria e Engenharia de Projeto LTDA. (2004). "*Análise em Serviço da Plataforma de Merluza (PMLZ-1)*", Technical Report (In Portuguese).

Griffin, M. J. (1996). *Handbook of Human Vibration*. Ed. Academic Press, London.

GTSTRUDL. (2009). Structural Design & Analysis Software, Release 29.1.

ISO 1940-1. *Mechanical Vibration. (2003). Balance Quality Requirements for Rotors in a Constant (Rigid) State. Part 1: Specification and Verification of Balance Tolerances*.

ISO 2631-1. *Mechanical Vibration and Shock. (1997). Evaluation of Human Exposure to Whole-body Vibration. Part 1: General Requirements*.

ISO 2631-2. *Mechanical Vibration and Shock. (1989). Evaluation of human exposure to whole-body vibration. Part 2: human exposure to continuous and shock-induced vibrations in buildings (1 to 80Hz)*.

Lenzen, K. H. (1996). *Vibration of Steel Joist Concrete Slab Floors*. In: Engineering journal, v.3(3), p. 133-136.

López, E. J. (2002). *Dinámica de Rotores*. Graduation Monography. Universidad Nacional del Comahue.

Milet, R. R., (2006). "*Análise Comparativa de Métodos de Cálculo para Fundações de Máquinas*", MSc Dissertation (In Portuguese), Civil Engineering Post-graduate Programme, Federal University of Pernambuco, UFPE, Pernambuco, PE, Brazil.

Murray, T. M., Allen, D. E. and Ungar, E. E. (2003). *Floor vibration due to human activity*, Steel design guide series, AISC, Chicago, USA.

Pereira, C. C. G. (2005). "*Curvas de Percepção e Conforto Humano para Vibrações Verticais*". MSc Dissertation (In Portuguese), Civil Engineering Post-graduate Programme, Federal University of Ouro Preto, UFOP, Minas Gerais, MG, Brazil.

Poulos, H. G.; Davis, E. H. (1980). *Pile Foundation Analysis and Design*. John Wiley & Sons Inc., New York.

Reiher, H. E, Meister, F. J. (1946). *The Effect of Vibration on people*. Translated from Forsch Geb, p 381-386, Ohio.

Rimola, B. D. (2010). "*Análise Dinâmica de Plataformas de Aço a partir da Consideração do Efeito da Interação Solo-Estrutura*", MSc Dissertation (In Portuguese), Civil Engineering Post-graduate Programme, PGECIV, State University of Rio de Janeiro, UERJ, Rio de Janeiro, RJ, Brazil.

Rimola, B. D. ; Silva, J. G. S. da ; Sieira, A. C. C. F. ; Lima, L. R. O. de ; Neves, L. F. da C. (2010a). Vibration Analysis of a Production Platform Induced by Mechanical Equipments. Proceedings of The Tenth International Conference on Computational Structures Technology, CST 2010, Valência, Spain. Civil-Comp Press, Edinburg. v. 1. p. 1-12.

Rimola, B. D ; Silva, J. G. S. da ; Sieira, A. C. C. F. ; Lima, L. R. O. de. (2010b). Vibration Analysis of an Oil Production Platform. Proceedings of the CILAMCE 2010: XXXI Iberian Latin American on Computational Methods in Engineering and MECOM 2010: IX Argentinean Congress on Computational Mechanics, CILAMCE 2010, Buenos Aires, Argentina. AMCA (Argentine Association for Computational Mechanics). v. XXIX. p. 7529-7540.

Silva, E. L. da. (2004). "*Dinâmica de Rotores: Modelo Matemático de Mancais Hidrodinâmicos*". MSc Dissertation (In Portuguese), Federal University Paraná. Paraná,PR, Brasil.

Souza, M. G. de; Cicogna, T. R.; Chiquito, A. J. (2007). "*Excitação dos modos normais de um sistema usando um motor desbalanceado*". Revista Brasileira de Ensaio de Física, v. 29, n. 1, p.5-10, Brazil.

Srinivasulu, P.; Vaidyanathan, C. V. (1976). *Handbook of Machine Foundations*. McGraw-Hill, New Delhi.

Terzaghi, K. (1955). *Evaluation of Coefficients of Subgrade Reaction*. Géotechnique, London, v. 4, nº 4, p. 297-326.

Vasconcelos, R. P. (1998). "*Atenuações de Vibrações em Lajes Nervuradas de Piso em Concreto Armado*". MSc Dissertation (In Portuguese), Civil Engineering Post-graduate Programme, Federal University of Rio de Janeiro, UFRJ, Rio de Janeiro, RJ, Brazil.

Winkler, E. (1867). "*Die Lehre von Elastizitat und Festigkeit*" (On Elasticity and Fixity), Dominicus, Prague.

Zhou, S.; Shi, J. (2001). *Active Balancing and Vibration Control of Rotating Machinery: A Survey*. The Shock and Vibration Digest - Sage Public ations, Vol. 33, No. 4, p. 361-371.

Vibration Analysis and Control - New Trends and Developments
Edited by Dr. Francisco Beltran-Carbajal

ISBN 978-953-307-433-7
Hard cover, 352 pages
Publisher InTech
Published online 06, September, 2011
Published in print edition September, 2011

This book focuses on the important and diverse field of vibration analysis and control. It is written by experts from the international scientific community and covers a wide range of research topics related to design methodologies of passive, semi-active and active vibration control schemes, vehicle suspension systems, vibration control devices, fault detection, finite element analysis and other recent applications and studies of this fascinating field of vibration analysis and control. The book is addressed to researchers and practitioners of this field, as well as undergraduate and postgraduate students and other experts and newcomers seeking more information about the state of the art, challenging open problems, innovative solution proposals and new trends and developments in this area.

INTECH
open science | open minds

InTech Europe
University Campus STeP Ri
Slavka Krautzeka 83/A
51000 Rijeka, Croatia
Phone: +385 (51) 770 447
Fax: +385 (51) 686 166
www.intechopen.com

InTech China
Unit 405, Office Block, Hotel Equatorial Shanghai
No.65, Yan An Road (West), Shanghai, 200040, China
中国上海市延安西路65号上海国际贵都大饭店办公楼405单元
Phone: +86-21-62489820
Fax: +86-21-62489821

IntechOpen